Biophysical Chemistry 135 (2008) 95–101

Contents lists available at ScienceDirect

Biophysical Chemistry

journal homepage: http://www.elsevier.com/locate/biophyschem

A new interpretation of eutectic behavior for distearoylphosphatidylcholine–cholesterol binary bilayer membrane

Nobutake Tamai, Maiko Uemura, Tetsuya Takeichi, Masaki Goto, Hitoshi Matsuki *, Shoji Kaneshina

Department of Life System, Institute of Technology and Science, The University of Tokushima, 2-1 Minamijosanjima-cho, Tokushima 770-8506, Japan
Department of Biological Science and Technology, Faculty of Engineering, The University of Tokushima, 2-1 Minamijosanjima-cho, Tokushima 770-8506, Japan

ARTICLE INFO

Article history:
Received 25 January 2008
Received in revised form 27 March 2008
Accepted 27 March 2008
Available online 4 April 2008

Keywords:
Cholesterol
Distearoylphosphatidylcholine
Eutectic behavior
Hexagonal lattice
Phase diagram

ABSTRACT

We investigated the thermotropic phase behavior of the distearoylphosphatidylcholine (DSPC)–cholesterol binary bilayer membrane as a function of the cholesterol composition (X_{ch}) by fluorescence spectroscopy using 6-propionyl-2-(dimethylamino)naphthalene (Prodan) and differential scanning calorimetry (DSC). The fluorescence spectra, each of which has a single maximum, showed that the wavelength at the maximum intensity (λ_{max}) changed depending on the bilayer state: ca. 440 nm for the lamellar gel (L'_β or L_β) and the liquid ordered (L_o) phases, ca. 470 nm for the ripple gel (P'_β) phase and ca. 490 nm for the liquid crystalline (L_α) phase, respectively. The transition temperatures were determined from the temperature dependences of the λ_{max} and endothermic peaks of the DSC thermograms. Both measurements showed that the pretransition disappears around $X_{ch}=0.035$. The constructed temperature–X_{ch} phase diagram indicated that the phase behavior of the binary bilayer membrane at $X_{ch}\leq 0.15$ is similar to that of general liquid–solid equilibrium for a binary system where both components are completely miscible in the liquid phase and completely immiscible in the solid phase. It was also revealed that the diagram has two characteristic points: a congruent melting point at $X_{ch}=0.08$ and a peritectic-like point at $X_{ch}=0.15$. The hexagonal lattice model was used for the interpretation of the phase behavior of the binary bilayer membrane. These characteristic compositions well correspond to the bilayer states in each of which cholesterol molecules are regularly distributed in the hexagonal lattice in a different way. That is, each composition of 0.035, 0.08 and 0.15 is nearly equal to that for the binary bilayer membrane which is entirely occupied with units, each composed of a cholesterol and 30 surrounding DSPC molecules within the next-next-next nearest neighbor sites (Unit (1:30): $L_\beta(1{:}30)$), with units, each of a cholesterol and 12 surrounding DSPC molecules within the next nearest sites (Unit (1:12): $L_\beta(1{:}12)$) or with units, each of a cholesterol and 6 surrounding DSPC molecules at the nearest neighbor sites (Unit (1:6): $L_\beta(1{:}6)$), respectively. Therefore, the eutectic behavior observed in the phase diagram was fully explainable in terms of a kind of phase separation between two different types of regions with different types of regular distributions of cholesterol. Further, the L_o phase was found in the higher X_{ch}-region ($X_{ch}>0.15$). No endothermic peak over the temperature range from 10 to 80 °C at $X_{ch}=0.50$ suggested that the single L_o phase can exist at $X_{ch}>0.50$.

1. Introduction

Cholesterol is a major and essential constituent of plasma membranes. In mammalian plasma membranes, cholesterol is found to be about 30% of the total lipid mass [1]. Cholesterol also plays an important role in a recent model for membrane structure, the so-called raft model [2]. This model represents the structural feature of heterogeneity in lipid membranes, and the origin of the heterogeneity is closely related to the presence of cholesterol. Therefore, the clarification of the role of cholesterol as a membrane component is indispensable for better understanding the functions, properties and structures of cell membranes. Considerable researches have been made for more than three decades and large amount of information on the role of the cholesterol is now available to us. Cholesterol and the relating matters in cell membranes have been described in some recent review articles [3–8] and a textbook edited by Yeagle [9].

Since the thermotropic and barotropic phase behavior of phospholipid bilayer membranes is intrinsically related to thermodynamic properties of the bilayer membrane [10–14], drawing phase diagrams for cholesterol–phospholipid binary bilayer membranes is useful to elucidate the effect of cholesterol on phospholipid bilayer membranes. There have been many studies dealing with the determination of phase boundaries for cholesterol–phospholipid binary systems using various experimental techniques such as neutron or X-ray scattering [15,16], differential scanning calorimetry (DSC) [17,18], fluorescence spectroscopy [19–21], dilatometry [22,23], EPR (ESR) or NMR [24–28]

* Corresponding author. Tel.: +81 88 656 7513; fax: +81 88 655 3162.
E-mail address: matsuki@bio.tokushima-u.ac.jp (H. Matsuki).

0301-4622/$ – see front matter © 2008 Elsevier B.V. All rights reserved.
doi:10.1016/j.bpc.2008.03.008

and others [29,30]. Most studies commonly showed that the incorporation of a good amount of cholesterol remarkably enhances the stability of the overall bilayer membrane. This stabilization causes the severe uncertainty of the bilayer phase transition at the same time, so the reported phase diagrams are more or less different from one another. This inconsistency indicates that different experimental methods can monitor different aspects of the phase behavior of the binary bilayer system. Lentz et al. [19] have early pointed out the importance of extensive investigation by the combination of several techniques, although the results might render an abstruse phase diagram in terms of thermodynamics.

The phase diagram that is most extensively accepted is probably that of the cholesterol/chain perduterated dipalmitoylphosphatidylcholine (d_{62}-DPPC) system given by Vist and Davis [25]. This is because the phase diagram is consistent with the calculation based on a thermodynamic and a simple microscopic model by Ipsen et al. [31]. These phase diagrams indicate some interesting features. One is that a two-phase region appears at relatively high compositions of cholesterol: a cholesterol-rich phase and a cholesterol-poor phase. The former phase is called liquid ordered (L_o) phase, which is characterized by high conformational order in the hydrocarbon chains like the gel state and relatively fast lateral diffusion. This phase separation is considered to be relevant to the formation of the heterogeneous structure of cell membranes. Another feature is that the cholesterol and the phospholipid molecules are as miscible even in the gel phase (i.e., a solid-like state) as in the liquid crystalline phase in the low cholesterol-composition region. Such miscibility is interesting, because even the binary mixtures of phosphatidylcholine analogues tend to exhibit immiscibility in the gel phase as their difference in the molecular structure, such as the hydrocarbon-chain length and the presence of chain unsaturation, becomes greater [32]. In general, physicochemical behavior in the low composition region, namely dilute region, is of greater importance because properties of an individual solute molecule in the binary mixture can be reflected more definitely. Probably, this view can be applied to also the cholesterol–phospholipid binary membrane, and at least it is reasonable to consider that the miscibility between cholesterol and phospholipid molecules essentially changes depending on the molecular structure of the phospholipid. Nevertheless, less attention has been paid to the phase behavior in the low composition region.

In the present study, we report the thermotropic phase behavior of distearoylphosphatidylcholine (DSPC)–cholesterol binary bilayer membrane investigated by means of DSC and fluorescence spectroscopy using 6-propionyl-2-(dimethylamino)naphthalene (Prodan) as a fluorescent probe. The DSC is highly sensitive to the conformational change of hydrocarbon chains (i.e., chain melting) in the bilayer. On the other hand, the Prodan fluorescence method is sensitive to the microscopic change near the hydrophilic surface in the bilayer [33]. Thus, the combination of the two disparate techniques allows us to observe the phase behavior of the system from different aspects. Much effort has been directed toward elucidating the phase behavior especially at low cholesterol compositions. In addition, we propose a novel interpretation of the phase diagram, including the L_o phase formed at high cholesterol compositions, which can explain the lateral distribution of cholesterol molecules in the bilayer membrane on the basis of a modified superlattice model [3].

2. Materials and methods

Synthetic DSPC (1,2-distearoyl-*sn*-glycero-3-phosphocholine) and cholesterol (5-cholesten-3β-ol) were purchased from Sigma-Aldrich Co. (St. Louis, MO) and used without further purification. The fluorescent probe of Prodan (6-propionyl-2-(dimethylamino) naphthalene) was obtained from Molecular Probes Inc. (Eugene, OR). Water used in preparing sample solutions was distilled twice from dilute alkaline permanganate solution. The multilamellar vesicle (MLV) suspensions of DSPC and mixture of DSPC and cholesterol were prepared by referring to the Bangham's method [34] as follows. The stock solutions of DSPC/chloroform, cholesterol/chloroform and Prodan/ethanol were mixed and the mixed solution was dried in vacuum to remove all residual solvents. The resulting dry film was dispersed by the addition of a given amount of distilled water. The suspension obtained was stirred using a vortex mixer and sonicated for ca. 5 min at a temperature several degrees higher than the main-transition temperature of the DSPC bilayer membrane to form a homogeneous MLV suspension, which was translucent. The concentrations of DSPC and Prodan were fixed at 1 mmol kg^{-1} and 2 μmol kg^{-1} (i.e., molar ratio of DSPC to Prodan is 500:1), respectively. In our previous study [35], it has been verified from the DSC thermogram of the Prodan–DSPC bilayer membrane that such a slight amount of Prodan has no significant influence on the thermotropic phase behavior of the DSPC bilayer membrane. The cholesterol composition (X_{ch}) in the bilayer membrane was varied from 0 to 0.50 in mole fraction. Here, X_{ch} is defined as $m_{ch}/(m_{DSPC}+m_{ch})$, where m_{ch} and m_{DSPC} represent the molalities of cholesterol and DSPC in the sample solution, respectively.

The fluorescence measurements were performed using a fluorescence spectrophotometer (Hitachi Model F-3010) at constant temperatures ranging from 30 to 80 °C. Temperature was controlled within an accuracy of 0.1 °C by circulating thermostated water from a temperature-regulated water bath. The excitation wavelength was 361 nm and the emission spectra were recorded in the range of 400–600 nm.

Differential scanning calorimetry (DSC) measurements were carried out by means of high-sensitivity differential scanning calorimeter (MicroCal MCS). The heating rate was 0.33 °C min^{-1} and the temperature range was from 10 to 80 °C. The temperatures and enthalpy changes associated with the phase transitions were determined from endothermic peaks in the DSC thermograms by use of a data-analyzing software ORIGIN supplied by MicroCal.

3. Results and discussion

3.1. Fluorescence measurements for DSPC bilayer membrane

Fig. 1 shows the emission spectra of Prodan in the DSPC bilayer membrane at every 2 °C from 48 to 60 °C. Every spectrum has a single maximum, and the wavelength at the maximum fluorescence intensity (λ_{max}) shifts from ca. 440 to ca. 490 nm with increasing temperature. It is known that the λ_{max} is sensitive to the polarity of microscopic environment around the fluorescent probe molecule. We also have previously confirmed that the λ_{max} values of Prodan in various solvents vary depending on the dielectric constant of the solvent and that there is a good correlation between the dielectric constant and the λ_{max} value [33]. Therefore, the shift of the λ_{max} of

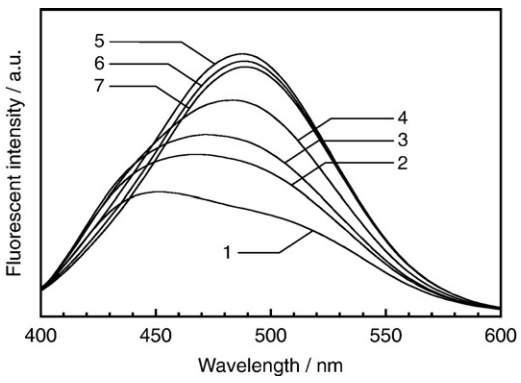

Fig. 1. Emission spectra of Prodan in DSPC bilayer membrane at every 2 °C from 48 to 60 °C: spectrum 1, 48 °C; 2, 50 °C; 3, 52 °C; 4, 54 °C; 5, 56 °C; 6, 58 °C; 7, 60 °C.

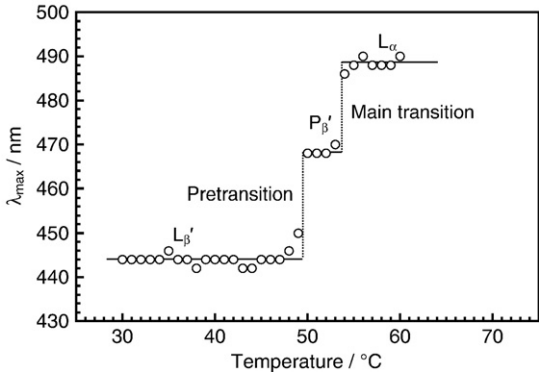

Fig. 2. Temperature dependence of wavelength at maximum fluorescence intensity for DSPC bilayer membrane. Two discontinuous changes indicated by dashed lines correspond to the pre- and main transitions.

Prodan in the DSPC bilayer membrane with increasing temperature is attributed to the change in the polarity around the Prodan molecules. The temperature dependence of the λ_{max} is shown in Fig. 2. There are two abrupt changes in the λ_{max} vs. temperature curve: one is from ca. 440 to ca. 470 nm in the vicinity of 50 °C and the other from ca. 470 to ca. 490 nm at almost 54 °C. The lower and higher temperatures are nearly equal to those of the pretransition between the lamellar gel (L_β') and ripple gel (P_β') phases and the main transition between the P_β' and liquid crystalline (L_α) phases for the DSPC bilayer membrane, respectively. This means that the local polarity around the Prodan molecules in the bilayer well corresponds to the phase state of the bilayer. Okamura et al. [36] have proposed a zone model for phosphatidylcholine bilayer membranes, where the local polarity in the bilayer steeply varies in the interfacial region between the hydrophilic surface and the hydrophobic core. Therefore, the change in the local polarity around the Prodan molecules is probably caused by the change of the vertical distribution of Prodan molecules in the bilayer with the thermotropic phase transitions, and the discontinuous change in the λ_{max} vs. temperature curve corresponds to the bilayer phase transitions.

3.2. Fluorescence measurements for DSPC–cholesterol binary bilayer membranes

The temperature dependences of the λ_{max} at various X_{ch} are shown in Fig. 3. At X_{ch}=0.005, the λ_{max} vs. temperature curve was almost similar to that for the pure DSPC bilayer. The pretransition became much more obscure with increasing X_{ch}: the stepwise λ_{max} shift progressively disappeared with X_{ch}. Such change in the λ_{max} is no longer detectable at X_{ch}=0.04, indicating that the pretransition vanishes in the vicinity of the composition. The behavior of the λ_{max} suggests that the pretransition does not correspond to the transition from the L_β' to the P_β' phase like the *pure* DSPC bilayer in the *binary* bilayers, which will be elucidated from the temperature–X_{ch} phase diagram later.

As the X_{ch} increases further, an influence on the main transition was clearly observed in the curves. At X_{ch}=0.06, the abrupt λ_{max} shift took place at almost 54 °C, but the λ_{max} jump itself did not reach around 490 nm. Subsequent heating over a few degrees brought about moderate increase in the λ_{max} and then the λ_{max} value became almost constant at about 490 nm as is seen in the plateau region of the λ_{max}. The temperature interval of the moderate change in the λ_{max} was extended with increasing X_{ch} up to 0.08. The region of the moderate change in the λ_{max} corresponds to some two-phase region as revealed in the following section. Interestingly, such moderate change in the λ_{max} once became smaller at X_{ch}=0.09 and 0.10, and the gradual change appeared again in $0.11 \le X_{ch} \le 0.15$ over much wider temperature range. In such X_{ch} range, the λ_{max} jump at 54 °C was rather depressed than that for X_{ch}=0.08. The λ_{max} increased gradually up to about 475 nm with succeeding heating, which was followed by another sudden shift of the λ_{max} up to the plateau region at 490 nm. At $X_{ch} \ge 0.15$, a gradual increase of the λ_{max} started around 54 °C instead of the steep rise, and it was followed by an abrupt shift up to about 465 nm at a higher temperature. After a slight increase in the λ_{max} over a temperature range of about 5 °C, the λ_{max} shifted abruptly once again to 490 nm. The temperature interval of the former gradual increase in the λ_{max} starting at about 54 °C was much extended with increasing X_{ch} up to 0.30. At first glance, the two steep λ_{max} changes in the λ_{max} vs. temperature curve appear to correspond to bilayer transitions. However, we regarded the points at which the λ_{max} started to increase from 440 nm and reached 490 nm as the beginning and completion of the transition from the gel phase to the liquid crystalline phase, respectively, taking into account that the λ_{max} values

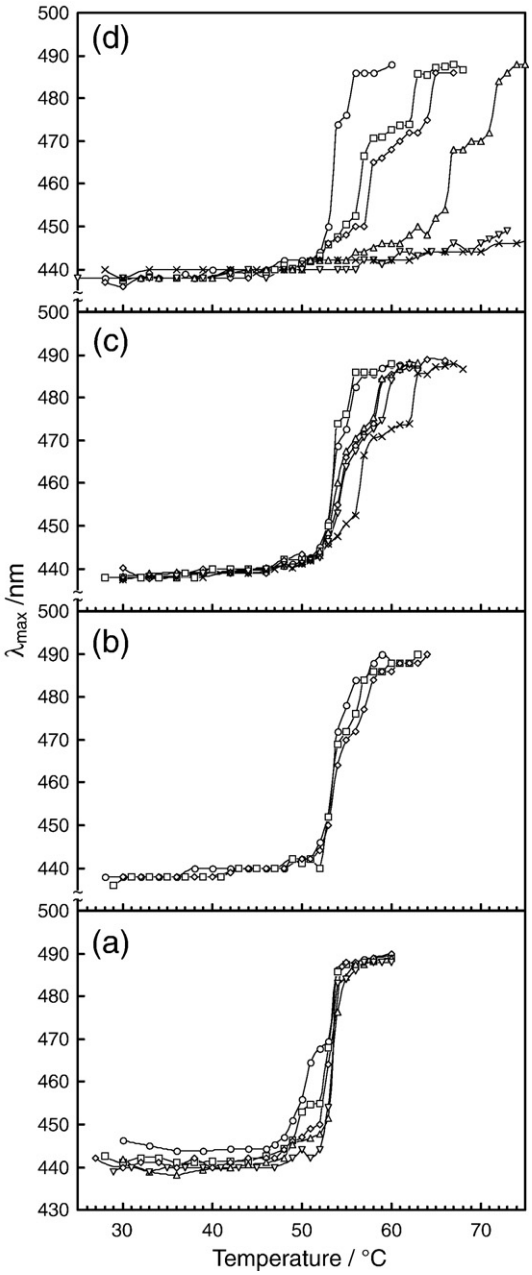

Fig. 3. Temperature dependence of wavelength at maximum fluorescence intensity, λ_{max}, for various DSPC-cholesterol binary bilayer membranes at different cholesterol compositions from 0.005 to 0.50: (a) ○, 0.005; □, 0.01; ◇, 0.02; △, 0.03; ▽, 0.04; (b) ○, 0.06; □, 0.07; ◇, 0.08; (c) ○, 0.09; □, 0.10; ◇, 0.11; △, 0.12; ▽, 0.14; ×, 0.15; (d) ○, 0.10; □, 0.15; ◇, 0.20; △, 0.30; ▽, 0.40; ×, 0.50.

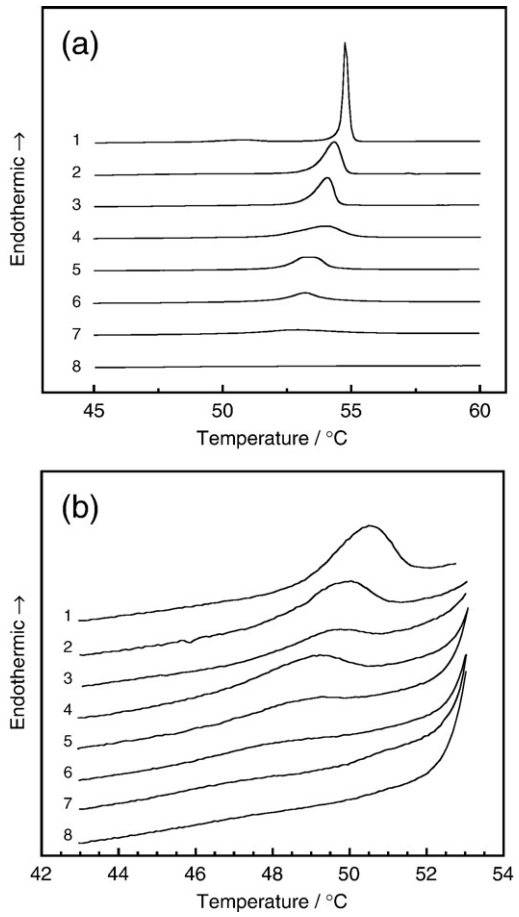

Fig. 4. DSC thermograms of pure DSPC bilayer and DSPC–cholesterol binary bilayer membranes at different cholesterol compositions. Each thermogram is vertically shifted to avoid overlapping one another. (a) 1, $X_{ch}=0$; 2, $X_{ch}=0.02$; 3, $X_{ch}=0.04$; 4, $X_{ch}=0.07$; 5, $X_{ch}=0.10$; 6, $X_{ch}=0.14$; 7, $X_{ch}=0.20$; 8, $X_{ch}=0.40$; (b) 1, $X_{ch}=0$; 2, $X_{ch}=0.005$; 3, $X_{ch}=0.010$; 4, $X_{ch}=0.015$; 5, $X_{ch}=0.020$; 6, $X_{ch}=0.025$; 7, $X_{ch}=0.030$; 8, $X_{ch}=0.035$.

of 440 and 490 correspond to the gel and liquid crystalline phases of the bilayer. Further, we considered that the wide temperature difference between the onset and completion of the transition is also attributable to another kind of two-phase region. At $X_{ch} \geq 0.40$, no significant increase in the λ_{max} was observed in the λ_{max} vs. temperature curves.

3.3. DSC measurements for DSPC–cholesterol binary bilayer membranes

Fig. 4(a) demonstrates DSC thermograms of the DSPC–cholesterol binary bilayer membranes at different X_{ch}. Here, the thermograms in the vicinity of the pretransitions at X_{ch} below 0.035 are magnified in Fig. 4(b). The thermogram of the pure DSPC bilayer exhibited two endothermic peaks corresponding to the pre- and main transitions at 50.5 °C and 54.8 °C, respectively. The endothermic peak of the main transition became smaller and broader with increasing X_{ch}. No endothermic peak was observed at $X_{ch}=0.50$. Regarding the pre-transition, the peak also became smaller with increasing X_{ch} and disappeared at $X_{ch}=0.035$.

In Fig. 5, the enthalpy changes (ΔH) of the pre- and main transitions are plotted against X_{ch}. The ΔH value of the main transition decreased linearly with increasing X_{ch} and reached zero at about $X_{ch}=0.50$. Similar behavior has been reported by McMullen et al. [37,38], and they found that there was actually no trace of the peak representing the main transition on the DSC thermogram for the binary bilayer at $X_{ch}=0.50$. Since the thermodynamic quantity changes of the main transition of a phospholipid bilayer membrane is attributable to the *trans–gauche*

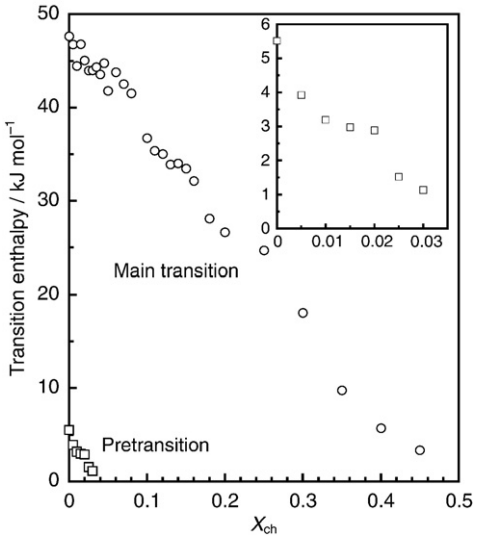

Fig. 5. The dependence of enthalpy changes on cholesterol composition for pre- and main transitions. The inset is a magnification of region in the vicinity of pretransition.

conformational change of the hydrocarbon chains (i.e., chain melting), the decrease in ΔH with increasing X_{ch} indicates that the incorporation of cholesterol into the bilayer membrane restrains the conformational change. We also observed a similar decrease in the ΔH value of the pretransition with X_{ch}. The ΔH value became zero at about $X_{ch}=0.035$. The composition of the pretransition disappearance was well consistent with that obtained from the fluorescence measurements.

The peak temperatures of the pre- and main transitions are plotted against X_{ch} in Fig. 6. The main-transition temperature decreased with increasing X_{ch} up to about 0.15, whereas it increased slightly with X_{ch} above 0.30. Hence, the transition temperature vs. X_{ch} curve had a shallow minimum around $X_{ch}=0.20$. Taking into account that the variation of the temperature was small for all the remarkably broad and small endothermic peak of the main transition, however, we regarded the temperature as virtually constant at $X_{ch} \geq 0.15$, which is clarified on the phase diagram later. The solid line in Fig. 6 represents the relationship between the transition temperature T and X_{ch}

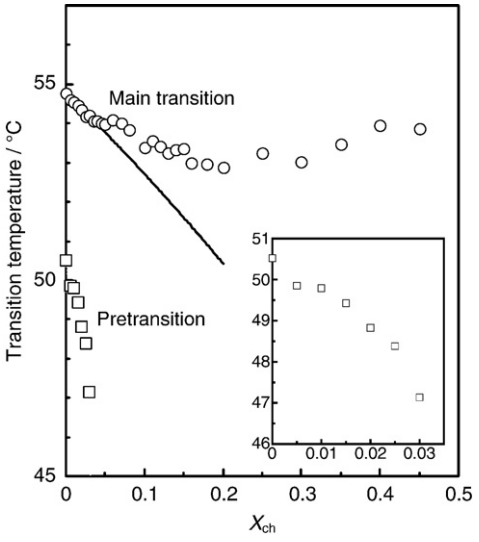

Fig. 6. The dependence of peak temperatures on cholesterol composition for pre- and main transitions. The inset is a magnification of region in the vicinity of pretransition.

calculated by use of the equation of liquid–solid phase equilibrium for an ideal binary solution:

$$\ln(1 - X_{ch}) = \frac{\Delta H^\circ}{R}\left(\frac{1}{T} - \frac{1}{T^\circ}\right)$$

where ΔH° and T° are an enthalpy change of a phase transition and a transition temperature for a pure bilayer membrane, respectively, and R is the gas constant. Here, we used $\Delta H^\circ = 45.2$ kJ mol^{-1} and $T^\circ = 327.93$ K for the DSPC bilayer to draw the curve of the phase equilibrium between the P_{β}' and the L_α phases on the assumption of the perfect miscibility of cholesterol and phospholipid molecules in the L_α phase and the perfect immiscibility of them in the P_{β}' phase. The experimental data were in good agreement with the transition temperature calculated using the equation at lower $X_{ch} \leq 0.04$. This suggests that the pure DSPC bilayer, which serves as a solvent, *freezes out* when the phase transition from the L_α phase to the P_{β}' phase takes place in the low X_{ch}-region, and the cholesterol and DSPC molecules are almost immiscible in the P_{β}' phase in the X_{ch}-region. Vist and Davis [25] have demonstrated for d_{62}-DPPC–cholesterol binary bilayer membrane that the cholesterol and d_{62}-DPPC molecules are partially or completely miscible at X_{ch} below about 0.07. This suggests that the difference in hydrocarbon-chain length only by two carbon–carbon bonds greatly affects the miscibility of the cholesterol in the phospholipid membranes.

The greater depression of the pretransition temperature compared to the main-transition temperature was observed and the pretransition itself abolished at $X_{ch} = 0.035$. Although the thermodynamic consideration can be applied to the depression of the pretransition temperature on the basis of the partitioning of the cholesterol molecules into the L_{β}' and P_{β}' phases [39], the difference in the membrane structure between the L_{β}' and P_{β}' phases cancels out each other progressively with increasing X_{ch}, judging from the X_{ch}-dependence of the ΔH value. So we introduced a new idea by use of a hexagonal lattice model to explain the miscibility and immiscibility of the cholesterol and DSPC molecules in the liquid crystalline and gel phases, which is discussed on the temperature–X_{ch} phase diagram later.

The peak width at half height ($\Delta T_{1/2}$) of the endothermic peak for the main transition is plotted against X_{ch} in Fig. 7. The peak of the pure DSPC bilayer membrane was quite sharp and the $\Delta T_{1/2}$ value was 0.27 °C. The slight addition of cholesterol caused the apparent broadening of the peak (e.g., $\Delta T_{1/2} = 0.59$ °C at $X_{ch} = 0.005$). The $\Delta T_{1/2}$ increased with increasing X_{ch} and it reached about 1 °C at $X_{ch} = 0.05$. At $X_{ch} = 0.06$, the $\Delta T_{1/2}$ suddenly jumped to about 2 °C. Subsequently, it decreased abruptly down to almost 1 °C at $X_{ch} = 0.10$ and it remained almost constant at X_{ch} up to 0.15. At $X_{ch} \geq 0.15$, the $\Delta T_{1/2}$ value markedly increased with increasing X_{ch} and finally reached more than 12 °C at $X_{ch} = 0.45$. The above characteristic compositions of 0.06, 0.10 and 0.15 were well consistent with those at which the behavior of the λ_{max} vs. temperature curve in Fig. 3 changed: (1) a temperature interval of a few degrees after the abrupt λ_{max} shift at 54 °C at $X_{ch} = 0.06$, (2) relatively sharp shift of the λ_{max} at $X_{ch} = 0.09$ and 0.10, (3) the remarkable extension of the temperature range for the λ_{max} increase at $X_{ch} \geq 0.15$. A broad endothermic peak is generally regarded as responsible for a decrease in the cooperativity of lipid molecules in bilayer phase transitions [32]. McMullen et al. have reported for phospholipid–cholesterol binary bilayer membranes [18,37,38] that the endothermic peak at the main transition, which usually appears as a single peak, consists of two overlapping components, a sharp peak and a broad peak corresponding to the chain melting of phospholipids in a cholesterol-poor region and in a cholesterol-rich region, respectively. They pointed out for the DPPC–cholesterol binary membrane [18] that the variation of the $\Delta T_{1/2}$ value of the overall endothermic peak is not necessarily relevant to the two-phase equilibrium of the binary bilayer membranes. However, taking account of the above good coincidence of the results between the DSC and fluorescence measurements, we can say that the sharpening and broadening of the overall endothermic peak are closely related to the extent of the two-phase equilibrium.

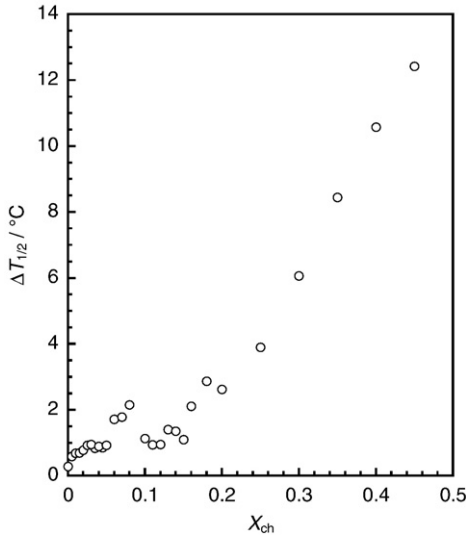

Fig. 7. The dependence of peak width at half height on cholesterol composition for endothermic peak of main transition.

3.4. T–X_{ch} phase diagram of DSPC–cholesterol binary bilayer membrane

In order to reveal the phase behavior of the DSPC–cholesterol binary bilayer membrane, we constructed the temperature–X_{ch} phase diagram from the results of the fluorescence and DSC measurements. The constructed temperature–X_{ch} phase diagram is shown in Fig. 8. Here, we use a term of L_α phase as a synonym of liquid disordered (L_d) phase which is generally used for membranes containing cholesterol. Similarly, we use the gel phase as the solid ordered (S_o) phase and the main transition as the phase transition between the S_o and L_d phases. We immediately noticed two characteristic features in the phase diagram. One is that the phase diagram is essentially similar to those representing solid–liquid equilibria of binary systems where both components are completely miscible in the liquid phase and completely immiscible in the solid phases. The good agreement between the main-transition temperature curve and an ideal freezing–depression curve at low X_{ch} in Fig. 6 supports the above view. Another is that the diagram has one clear congruent melting point (point X in Fig. 8) and one peculiar melting point like a peritectic point (point Y in Fig. 8). Such a phase diagram is obtained for solid–liquid phase equilibrium of a binary mixture where the two components produce a new compound in the solid phase stoichiometrically. This finding means that a cholesterol molecule interacts with some DSPC molecules to form a complex which behaves as a third chemical species in the gel phase. It has been demonstrated that there are discontinuous changes of some membrane properties at specified X_{ch} [3,40–42], which confirms that there really exist such specific interaction between cholesterol and phospholipid molecules. According to the so-called superlattice model proposed by Somerharju et al. [3], the discontinuous changes are regarded as an experimental evidence for the regular distribution of cholesterol in the membrane. This means that the binary bilayer membrane in which cholesterol regularly distributed is in the most stable state in terms of the free energy of the membrane [3]. This may also imply that an irregular distribution will possibly give rise to some distortion in the morphological structure of the vesicles, which leads to the instability of the binary bilayer membranes. Here, we considered for the DSPC–cholesterol binary bilayer membrane that the regular distribution is maintained at any X_{ch}, and then a fundamental unit in the regular distribution can behave as a complex of the regular structure with the same stoichiometric composition. The complex phase behavior given in Fig. 8 can be explained from the combination of the general

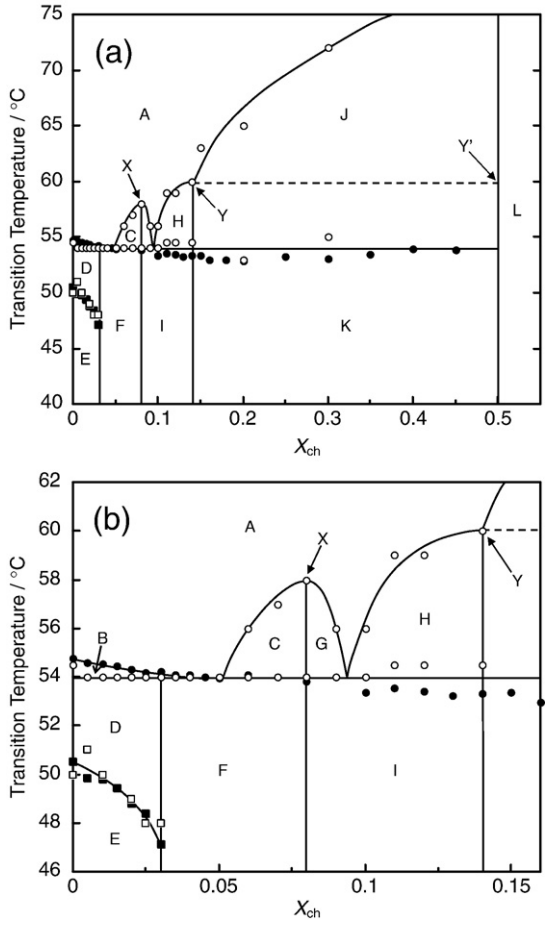

Fig. 8. Phase diagram for DSPC–cholesterol binary bilayer membrane: (a) the diagram in X_{ch} range from 0 to 0.50 and (b) magnified diagram in X_{ch} range from 0 to 0.16. Open and closed symbols mean the data from fluorescence and DSC measurements, respectively. Each area designated by an alphabet is assigned as follows: A, L_α; B, $L_\alpha+P'_\beta$; C, $L_\alpha+L_\beta$ (1:12); D, $P'_\beta+L_\beta$ (1:30); E, $L'_\beta+L_\beta$ (1:30); F, L_β (1:30)+L_β (1:12); G, $L_\alpha+L_\beta$ (1:12); H, $L_\alpha+L_\beta$ (1:6); I, L_β (1:12)+L_β (1:6); J, $L_\alpha+L_o$; K, L_β (1:6)+L_o; L, L_o.

thermodynamics of liquid–solid phase equilibrium and the superlattice model for regular distribution of cholesterol in binary bilayer membranes.

Fig. 9 illustrates various types of units based on the hexagonal lattice. An open circle on the lattice point in the figure represents a DSPC molecule and a closed circle does a cholesterol molecule. Although the superlattice model is often represented by molecular depiction where one lattice point is occupied with either a cholesterol molecule or one hydrocarbon chain of the phospholipid molecule [41], we adopted the occupancy of one molecule in a lattice point taking into account that the cross sectional areas of a fully extended hydrocarbon chain, a cholesterol molecule and a phosphatidylcholine molecule are roughly estimated to be 0.20, 0.40 and 0.55–0.70 nm^2 (depending on X_{ch}) on insoluble monolayers or mixed monolayers, respectively [43–46]. When the bilayer surface is entirely occupied with Units (1:30), each of which is composed of one cholesterol molecule and 30 surrounding DSPC molecules within the next–next–next nearest neighbor sites, the X_{ch} value is equal to 0.032. The composition is very close to that at which the pretransition nearly disappears. It is known that an addition of small quantity of cholesterol into the gel phases (i.e., the L'_β and P'_β phases) of pure phospholipid bilayer membranes induces the orientation of the phospholipid molecules normal to the bilayer surface [47] and reduces the static undulation of the bilayer surface in the P'_β phase [15,48]. That is, the incorporation of cholesterol in the gel phase of the DSPC bilayer causes the conversion of both the L'_β and P'_β phases into the L_β phase, which results in the complete disappearance of the pretransition around $X_{ch}=0.035$, corresponding approximately to the whole occupancy with Units (1:30) on the bilayer surface. This means that the effect of cholesterol spreads over the DSPC molecules within Unit (1:30), and that the DSPC molecules in Unit (1:30) become the L_β state (hereafter referred as L_β (1:30)) below the main-transition temperature. The other characteristic compositions, ca. 0.08 (at the congruent melting point X in Fig. 8) and 0.15 (at the peritectic-like point Y in Fig. 8), are nearly equal to those when the bilayer surface is entirely occupied with Units (1:12), each of a cholesterol and 12 surrounding DSPC molecules within the next nearest sites and with Units (1:6), each of a cholesterol and 6 surrounding DSPC molecules at the nearest neighbor sites, respectively. The DSPC molecules involved in each unit are probably in an L_β-like state below the main-transition temperature (hereafter referred as L_β (1:12) and L_β (1:6)) on the analogy of the L_β(1:30) state. However, the L_β (1:12) and L_β (1:6) states are defined as different states in the thermodynamic properties from each other. Furthermore, it should be noted that the pure L_o phase appears as a single phase at $X_{ch}>0.50$. The composition confirms that the L_o phase can be formed by the 1:1 complex of cholesterol and DSPC.

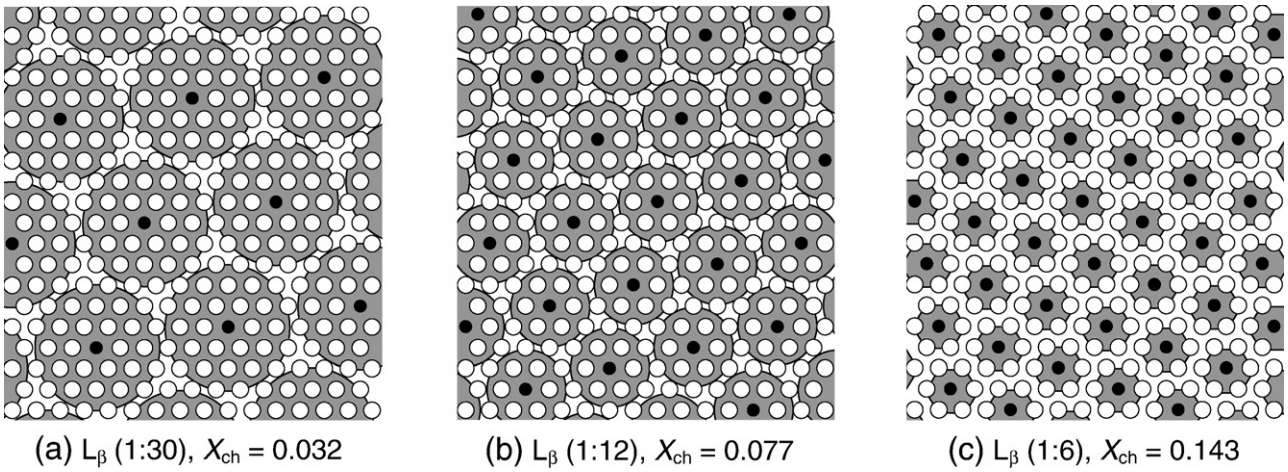

Fig. 9. Schematic illustration for various types of regular distribution of cholesterol in binary bilayer membranes based on hexagonal lattice model. Closed and open circle represent a cholesterol and a DSPC molecule, respectively. A fundamental unit is indicated as a dark shaded area around a cholesterol molecule in each panel: (a) Unit (1:30) includes 30 phospholipid molecules ($X_{ch}=0.032$), (b) Unit (1:12) 12 molecules ($X_{ch}=0.077$), (c) Unit (1:6) 6 molecules ($X_{ch}=0.143$).

We assigned the phase states for each area in the phase diagram (Fig. 8) according to the above consideration as follows: A, L_α; B, $L_\alpha+P_\beta'$; C, $L_\alpha+L_\beta$ (1:12); D, $P_\beta'+L_\beta$ (1:30); E, $L_\beta'+L_\beta$ (1:30); F, L_β (1:30)+L_β (1:12); G, $L_\alpha+L_\beta$ (1:12); H, $L_\alpha+L_\beta$ (1:6); I, L_β (1:12)+L_β (1:6); J, $L_\alpha+L_o$; K, L_β (1:6)+L_o; L, L_o. The binary bilayer membranes exist as five kinds of two-phase states at temperatures below the main-transition temperature and at $X_{ch}<0.50$ depending on X_{ch} (i.e., areas of D, E, F, I and K in Fig. 8). The membrane in the two-phase state is constituted by two different types of regions with the different regular distributions of cholesterol. For example, at $X_{ch}=0.10$ and a temperature below the main-transition temperature, the present bilayer membrane is composed of the regions separately formed by Units (1:12) and Units (1:6): the L_β (1:12) and L_β (1:6) phases coexist in the membrane.

In conclusion, we could construct the phase diagram of the DSPC–cholesterol binary bilayer membrane by using the methods of fluorescence spectroscopy and DSC. The characteristic compositions at which the bilayer behavior abruptly changes was reasonably explained in terms of thermodynamics of liquid–solid phase equilibrium for a binary mixture and hexagonal lattice model. The hexagonal lattice model is quite useful in understanding the interaction modes between the DSPC and cholesterol molecules in the gel phase. However, the phase diagram has not yet been perfect in respect of a lack of the line between points Y and Y′ in the higher X_{ch}-region. Unfortunately, we were not able to determine the line experimentally in this study because of the obscurity of the phase transition with the occurrence of the L_o phase. For the exact clarification of the phase behavior of phospholipid–cholesterol binary bilayer membranes, further investigation will be required, especially, in the X_{ch} range where the two phases coexist.

References

[1] H. Hauser, G. Poupart, Lipid structure, in: P.L. Yeagle (Ed.), The Structure of Biological Membranes, 2nd Ed., CRC Press, London, 2005, pp. 1–51.
[2] K. Simons, E. Ikonen, Functional rafts in cell membranes, Nature 387 (1997) 569–572.
[3] P. Somerharju, J.A. Virtanen, K.H. Cheng, Lateral organisation of lipids. The superlattice view, Biochim. Biophys. Acta 1440 (1999) 32–48.
[4] N.D. Ridgway, Interaction between metabolism and intracellular distribution of cholesterol and sphingomyelin, Biochim. Biophys. Acta 1484 (2000) 129–141.
[5] R.M. Epand, Do proteins facilitate the formation of cholesterol-rich domains? Biochim. Biophys. Acta 1666 (2004) 227–238.
[6] P.F.F. Almeida, A. Pokorny, A. Hinderliter, Thermodynamics of membrane domains, Biochim. Biophys. Acta 1720 (2005) 1–13.
[7] S.L. Veatch, S.L. Keller, Seeing spots: Complex phase behavior in simple membranes, Biochim. Biophys. Acta 1746 (2005) 172–185.
[8] J.R. Silvius, Partitioning of membrane molecules between raft and non-raft domains: Insights from model membrane studies, Biochim. Biophys. Acta 1746 (2005) 193–202.
[9] P.L. Yeagle (Ed.), The Structure of Biological Membranes, 2nd Ed., CRC Press, London, 2005.
[10] H. Ichimori, T. Hata, T. Yoshioka, H. Matsuki, S. Kaneshina, Thermotropic and barotropic phase transition on bilayer membranes of phospholipids with varying acyl chain-lengths, Chem. Phys. Lipids 89 (1997) 97–105.
[11] H. Ichimori, T. Hata, H. Matsuki, S. Kaneshina, Barotropic phase transitions and pressure-induced interdigitation on bilayer membranes of phospholipids with varying acyl chain-lengths, Biochim. Biophys. Acta 1414 (1998) 165–174.
[12] M. Kusube, H. Matsuki, S. Kaneshina, Thermotropic and barotropic phase transitions of *N*-methylated dipalmitoylphosphatidylethanolamine bilayers, Biochim. Biophys. Acta 1668 (2005) 25–32.
[13] M. Kusube, M. Goto, N. Tamai, H. Matsuki, S. Kaneshina, Bilayer phase transitions of *N*-methylated dioleoylphosphatidylethanolamines under high pressure, Chem. Phys. Lipids 142 (2006) 94–102.
[14] H. Matsuki, E. Miyazaki, F. Sakano, N. Tamai, S. Kaneshina, Thermotropic and barotropic phase transitions in bilayer membranes of ether-linked phospholipids with varying alkyl chain lengths, Biochim. Biophys. Acta 1768 (2007) 479–489.
[15] K. Mortensen, W. Pfeiffer, E. Sackmann, W. Knoll, Structural properties of a phosphatidylcholine–cholesterol system as studied by small-angle neutron scattering: ripple structure and phase diagram, Biochim. Biophys. Acta 945 (1988) 221–245.
[16] S. Karmakar, V.A. Raghunathan, S. Mayor, Phase behaviour of dipalmitoyl phosphatidylcholine (DPPC)–cholesterol membranes, J. Phys. Condens. Mater. 17 (2005) S1177–S1182.
[17] P. Laggner, K. Lohner, R. Koynova, B. Tenchov, The influence of low amounts of cholesterol on the interdigitated gel phase of hydrated dihexadecylphosphatidylcholine, Chem. Phys. Lipids 60 (1991) 153–161.
[18] T.P.W. McMullen, R.N. McElhaney, New aspects of the interaction of cholesterol with dipalmitoylphosphatidylcholine bilayers as revealed by high-sensitivity differential scanning calorimetry, Biochim. Biophys. Acta 1234 (1995) 90–98.
[19] B.R. Lentz, D.A. Barrow, M. Hoechli, Cholesterol–phosphatidylcholine interaction in multilamellar Vesicles, Biochemistry 19 (1980) 1943–1954.
[20] T. Parasassi, M.D. Stefano, M. Loiero, G. Ravagnan, E. Gratton, Cholesterol modifies water concentration and dynamics in phospholipid bilayers: a fluorescence study using Laudan probe, Biophys. J. 66 (1994) 763–768.
[21] O.P. Bonder, E.S. Rowe, Preferential interaction of fluorescent probe Prodan with cholesterol, Biophys. J. 76 (1999) 956–962.
[22] D.L. Melchior, F.J. Scavitto, J.M. Steim, Dilatometry of dipalmitoyllecithin–cholesterol bilayers, Biochemistry 19 (1980) 4828–4834.
[23] A.I. Greenwood, S. Tristram-Nagle, J.F. Nagle, Partial molecular volumes of lipids and cholesterol, Chem. Phys. Lipids 143 (2006) 1–10.
[24] D.J. Recktenwald, H.M. McConnell, Phase equilibria in binary mixture of phosphatidylcholine and cholesterol, Biochemistry 20 (1981) 4505–4510.
[25] M.R. Vist, J.H. Davis, Phase equilibria of cholesterol/dipalmitoylphosphatidylcholine mixtures: ^{2}H nuclear magnetic resonance and differential scanning calorimetry, Biochemistry 29 (1990) 451–464.
[26] M.B. Sankaram, T.E. Thompson, Interaction of cholesterol with various glycerophospholipids and sphingomyelin, Biochemistry 29 (1990) 10670–10675.
[27] M.B. Sankaram, T.E. Thompson, Modulation of phospholipid acyl chain order by cholesterol: a solid-state nuclear magnetic resonance study, Biochemistry 29 (1990) 10676–10684.
[28] L. Miao, M. Nielsen, J. Thewalt, J.H. Ipsen, M. Bloom, M.J. Zuckermann, O.G. Mouritsen, From lanosterol to cholesterol: structural evolution and differential effect on lipid bilayer, Biophys. J. 82 (2002) 1429–1444.
[29] P.F.F. Almeida, W.L.C. Vaz, T.E. Thompson, Lateral diffusion in the liquid phases of dimyristoylphosphatidylcholine/cholesterol bilayers: a free volume analysis, Biochemistry 31 (1992) 6739–6747.
[30] G.M. Troup, T.N. Tulenko, S.P. Lee, S.P. Wrenn, Estimating the size of laterally phase separated cholesterol domains in model membranes with Förster resonance energy transfer: a simulation study, Colloids Surf., B Biointerfaces 33 (2004) 57–65.
[31] J.H. Ipsen, G. Karlström, O.G. Mouritsen, H. Wennerström, M.J. Zuckermann, Phase equilibria in the phosphatidylcholine–cholesterol system, Biochim. Biophys. Acta 905 (1987) 162–172.
[32] R.N.A.H. Lewis, R.N. McElhaney, The mesomorphic phase behavior of lipid bilayers, in: P.L. Yeagle (Ed.), The Structure of Biological Membranes, 2nd Ed., CRC Press, London, 2005, pp. 53–120.
[33] M. Kusube, N. Tamai, H. Matsuki, S. Kaneshina, Pressure-induced phase transitions of lipid bilayers observed by fluorescent probes Prodan and Laurdan, Biophys. Chem. 117 (2005) 199–206.
[34] A.D. Bangham, J. DeGier, G.D. Grevill, Osmotic properties and water permeability of phospholipid liquid crystals, Chem. Phys. Lipids 1 (1967) 225–246.
[35] M. Kusube, H. Matsuki, S. Kaneshina, Effect of pressure on the Prodan fluorescence in bilayer membranes of phospholipids with varying acyl chain lengths, Colloids Surf., B Biointerfaces 42 (2005) 79–88.
[36] E. Okamura, M. Nakahara, NMR studies on lipid bilayer interfaces coupled with anesthetics and endocrine disruptors, in: A.G. Volkov (Ed.), Liquid Interfaces in Chemical, Biological, and Pharmaceutical Applications, Marcel Dekker, New York, 2000, pp. 775–805.
[37] T.P.W. McMullen, R.N.A.H. Lewis, R.N. McElhaney, Differential calorimetric study of the effect of cholesterol on the thermotropic phase behavior of a homologous series of linear saturated phosphatidylcholine, Biochemistry 32 (1993) 516–522.
[38] T.P.W. McMullen, R.N. McElhaney, Differential calorimetric study of the interaction of cholesterol with distearoyl and dielaidoyl molecular species of phosphatidylcholine, phosphatidylethanolamine, and phosphatidylserine, Biochemistry 36 (1997) 4979–4986.
[39] T. Hata, H. Matsuki, S. Kaneshina, Effect of local anesthetic on the phase transition temperatures of ether- and ester-linked phospholipid bilayer membranes, Colloids Surf., B Biointerfaces 18 (2000) 41–50.
[40] P.L.-G. Chong, Evidence for regular distribution of sterols in liquid crystalline phosphatidylcholine bilayers, Proc. Natl. Acad. Sci. U. S. A. 91 (1994) 10069–10073.
[41] J.A. Virtanen, M. Ruonala, M. Vauhkonen, P. Somerharju, Lateral organization of liquid-crystalline cholesterol–dimyristoylphosphatidylcholine bilayers. Evidence for domains with hexagonal and centered rectangular cholesterol superlattices, Biochemistry 34 (1995) 11568–11581.
[42] D. Tang, B.W. van der Meer, S.-Y.S. Chen, Evidence for a regular distribution of cholesterol in phospholipid bilayers from diphenylhexatriene fluorescence, Biophys. J. 68 (1995) 1944–1951.
[43] F. Müller-Landau, D.A. Cadenhead, Molecular packing in steroid–lecithin monolayers, Part I: Pure films of cholesterol, 3-doxyl-cholestane, 3-doxyl-17-hydroxyl-androstane, tetradecanoic acid and dipalmitoylphosphatidylcholine, Chem. Phys. Lipids 25 (1979) 299–314.
[44] F. Müller-Landau, D.A. Cadenhead, Molecular packing in steroid–lecithin monolayers, Part II: Mixed films of cholesterol with dipalmitoylphosphatidylcholine and tetradecanoic acid, Chem. Phys. Lipids 25 (1979) 315–328.
[45] I. Brzozowska, Z.A. Figaszewski, Interfacial tension of phosphatidylcholine–cholesterol system in monolayers at the air/water interface, Biophys. Chem. 95 (2002) 173–179.
[46] P. Dynarowicz-Łątka, K. Hąc-Wydro, Interactions between phosphatidylcholines and cholesterol in monolayers at the air/water interface, Colloids Surf., B Biointerfaces 37 (2004) 21–25.
[47] S. Matsuoka, S. Kato, I. Hatta, Temperature change of the ripple structure in fully hydrated dimyristoylphosphatidylcholine/cholesterol multibilayers, Biophys. J. 67 (1994) 728–736.
[48] J.B. Finean, Interaction between cholesterol and phospholipid in hydrated bilayers, Chem. Phys. Lipids 54 (1990) 147–156.